

Effect of dissipation fluctuations on anomalous velocity scaling in turbulence

Jens Eggers and Siegfried Grossmann

Fachbereich Physik der Philipps-Universität, Renthof 6, W-3550 Marburg, Federal Republic of Germany

(Received 16 November 1990; revised manuscript received 27 June 1991)

We introduce a one-dimensional model of a turbulent velocity field. It consists of a superposition of successively smaller eddies, forming a Cayley-tree-like structure. The randomness of the eddy decay is modeled by a multiplier distribution $p(s)$, whose parameters can be determined from experiment. In contrast to other cascade models, which are not stated in terms of the velocity field, every other quantity of the turbulent flow can now be calculated consistently. Scaling relations between the statistics of the velocity and the dissipation fields are shown to depend greatly on physical assumptions about the cascade. Specifically, we study the influence of the spatial coherence of eddies, and of the action of the viscous cutoff.

PACS number(s): 47.25.-c, 05.40.+j, 03.40.Gc

I. INTRODUCTION

We consider statistically homogeneous, isotropic turbulent flow in a finite volume of extension $2\pi L$ (mathematically periodically continued), stirred by the fluctuating velocity of the largest eddy. The statistical properties of the velocity field in high-Reynolds-number flow can be described by scaling relations such as

$$D(r) = \langle\langle |\mathbf{u}(\mathbf{x} + \mathbf{r}, t) - \mathbf{u}(\mathbf{x}, t)|^2 \rangle\rangle = b\epsilon^{2/3} r^{2/3}. \quad (1.1)$$

Here $\langle\langle \dots \rangle\rangle$ denotes the average over the statistical ensemble, and $\epsilon = \langle\langle v \partial_i u_j(x) \partial_i u_j(x) \rangle\rangle$ is the mean dissipation rate per unit mass. The range of validity of (1.1) is usually called the inertial subrange (ISR). At $r \approx 9\eta$ it merges into the viscosity-controlled viscous subrange (VSR), where $\eta = (\nu^3/\epsilon)^{1/4}$ is the Kolmogorov microscale. b is found to be 8.4 experimentally (see, e.g., [1,2]).

Though, within the present state of the art of measuring [3], there are no significant corrections to (1.1), it has been argued [4] that spatial fluctuations in the dissipation field

$$\epsilon(\mathbf{x}) = (\nu/2) [\partial_j u_i(\mathbf{x}) - \partial_i u_j(\mathbf{x})]^2$$

should induce corrections to (1.1). Such corrections to the classical scaling of Kolmogorov, Obukhov, von Weizsäcker, Heisenberg, and Onsager [5-9] are more apparent in the higher-order structure functions. So the scaling exponents $\zeta(m)$ of the longitudinal m th-order structure function

$$D_{\parallel}^{(m)}(r) = \langle\langle [\mathbf{u}(\mathbf{x} + \mathbf{r}, t) - \mathbf{u}(\mathbf{x}, t)]_{\parallel}^m \rangle\rangle \propto r^{\zeta(m)} \quad (1.2)$$

seem to differ visibly [3] for $m \gtrsim 6$ from

$$\zeta_{cl}(m) = m/3, \quad (1.3)$$

as found in the classical theory. Obukhov's argument is that the statistics of the velocity difference $\mathbf{v}(\mathbf{r}, \mathbf{x}) = \mathbf{u}(\mathbf{x} + \mathbf{r}) - \mathbf{u}(\mathbf{x})$ should depend on $\epsilon(\mathbf{x})$ averaged over a sphere of radius r ,

$$\epsilon_r(\mathbf{x}) = \frac{3}{4\pi r^3} \int_{V_r} \epsilon(\mathbf{x} + \mathbf{y}) dV(\mathbf{y}). \quad (1.4)$$

So typical velocity differences may be approximated by $v(r, \mathbf{x}) \approx \epsilon_r^{1/3}(\mathbf{x}) r^{1/3}$, giving

$$D_{\parallel}^{(m)}(r) = b_{\parallel}^{(m)} \langle\langle [\epsilon_r(\mathbf{x})]^{m/3} \rangle\rangle r^{m/3}. \quad (1.5)$$

One thus has shifted the problem of calculating $\zeta(m)$ to the study of the spatial fluctuations of $\epsilon(\mathbf{x})$.

Although the dissipation field $\epsilon(\mathbf{x})$ is completely defined in terms of the velocity field, one usually introduces separate and independent models for the $\epsilon(\mathbf{x})$ distribution. There are various such models, (see [4,10,11-14] and references cited therein). The following cascade model, first introduced by Yaglom [14,11] and recently used for diffusion on random Cayley trees [15], allows for a unifying description of the different distributions. A particular realization of $\epsilon_{r/2}$ is obtained from ϵ_r by multiplication with a random variable Y . The Y 's of the successive cascade steps are assumed to be independent, but their distributions are assumed to be the same. Then every ϵ_r can be written as the product of independent random variables

$$\epsilon_r = \left[\prod_{i=1}^{n_r} Y_i \right] \epsilon_L. \quad (1.6)$$

ϵ_L is the dissipation rate averaged over some largest length L . The number n_r of Y factors is $n_r = \log_2(L/2r)$. This gives

$$\langle\langle \epsilon_r^q \rangle\rangle = \epsilon_L^q \langle Y^q \rangle^{n_r} = \epsilon_L^q (L/2r)^{f(q)}, \quad (1.7)$$

with

$$f(q) = \log_2(\langle Y^q \rangle). \quad (1.8)$$

Note that the exponent in (1.7) per construction depends only on the distribution of Y and is independent of the number of cascade steps. Therefore $f(q)$ cannot be deduced from the central-limit theorem, even for $n_r \rightarrow \infty$, as it seems to be claimed by Yaglom [14,11]. For a recent review on the properties of $f(q)$ see [16].

Combining (1.7) and (1.5), one obtains the desired corrections to classical scaling

$$\delta\zeta(m) = \zeta(m) - m/3 = -f(m/3). \quad (1.9)$$

$f(2)$ is the exponent of the ϵ correlations, usually denoted as μ ,

$$\langle\langle [\epsilon(\mathbf{x}) - \epsilon][\epsilon(\mathbf{x} + \mathbf{r}) - \epsilon] \rangle\rangle \propto \epsilon^2 (r/L)^{-\mu}. \quad (1.10)$$

So one recovers the well-known formula [17,18]

$$\mu = 2 - \zeta(6). \quad (1.11)$$

$f(q)$ may be any convex function with

$$f(0) = f(1) = 0. \quad (1.12)$$

$f(1) = 0$ follows from the obvious condition $\langle\langle \epsilon_r \rangle\rangle = \epsilon$ and is equivalent to $\zeta(3) = 1$ according to (1.9) and is compatible with the Kolmogorov structure equation [1,19]; see also Sec. VI.

There is no obvious reason why the exponents $f(q)$ should be easier to evaluate than the original exponents $\zeta(m)$. Attempts have been made to calculate $f(2)$ from a polymer analogy [20], but an accepted derivation from the Navier-Stokes equation is still lacking. We therefore adopt the following pragmatic view to summarize the different functional forms proposed for $f(q)$.

It would be simplest to assume that $f(q)$ is a linear function in q . Together with (1.12) this gives $f(q) \equiv 0$ and one retains (1.3). The Novikov-Stewart or β model [21,17] amounts to weakening (1.12) and to assuming that (still linear)

$$f(q) = \mu(q - 1). \quad (1.13)$$

For $\mu > 0$, (1.13) gives corrections to scaling, but contains the flaw of violating the obvious relation $f(0) = 0$. If one wants to do better, one has to fit a polynomial of second order,

$$f(q) = \mu q(q - 1)/2. \quad (1.14)$$

This is the famous log-normal model of Kolmogorov [10]. Still another form of $f(q)$ is

$$f(q) = \log_2[\kappa(1/2)^{1-q} + (1 - \kappa)], \quad \kappa = 0.125, \quad (1.15)$$

as suggested by Benzi *et al.* [22].

A rather general insight into the physical origin of scaling corrections $\delta\zeta(m)$ was obtained in [15]. Whenever the scaling factors Y are not fixed but distributed, there are corrections $\delta\zeta(m)$. For smaller m it is the width $\langle(\log_2 Y - \langle\log_2 Y\rangle)^2\rangle / \langle\log_2 Y\rangle^2$ of the distribution that determines the correction irrespective of any details of $p(Y)$. For large m the correction becomes linear again in m , the slope being dominated now by $\log_2 Y_{\max}$ instead of $\langle\log_2 Y\rangle$ as for small m .

Other scaling exponents that indicate deviations from classical scaling are the exponents $g(q)$ of the one-point dissipation-rate moments

$$\langle\langle [\epsilon(\mathbf{x})]^q \rangle\rangle / \langle\langle \epsilon(\mathbf{x}) \rangle\rangle^q \propto \text{Re} \epsilon_\lambda^{g(q)}. \quad (1.16)$$

Cascade models predict that the exponent of skewness

$$S = \langle\langle (\partial_1 u_1)^3 \rangle\rangle / \langle\langle (\partial_1 u_1)^2 \rangle\rangle^{3/2} \propto \text{Re} \epsilon_\lambda^{\mu_S} \quad (1.17)$$

and of kurtosis

$$K = \langle\langle (\partial_1 u_1)^4 \rangle\rangle / \langle\langle (\partial_1 u_1)^2 \rangle\rangle^2 \propto \text{Re} \epsilon_\lambda^{\mu_K} \quad (1.18)$$

are special cases: $\mu_S = g(\frac{3}{2})$, and $\mu_K = g(2)$.

All models described so far rest on *ad hoc* assumptions about the interrelation between velocity and dissipation fluctuations, and are stated in terms of the dissipation field. Instead, the model we present here consists of an ensemble of velocity fields. Any other quantity, such as, for example, the dissipation field, is then uniquely determined. This approach is fundamentally different from the one taken, for example, in [13], although formally the cascade construction might look similar. Once the ensemble of $\mathbf{u}(\mathbf{x})$ fields is specified, there is no freedom anymore in making assumptions like (1.5), or as in [17,22,23].

The main point of this paper is to demonstrate that indeed a whole variety of *different* scaling laws is consistent with a hierarchical structure of eddies. The result depends on assumptions about the coherence of eddies, and on the nature of the viscous cutoff. To settle these questions, detailed dynamical, i.e., Navier-Stokes-motivated, information is needed.

Given a series of velocity scaling exponents $\zeta(m)$ we obtain $\mu = 0$ if the eddies are coherent in space. If the eddies fluctuate in space, $\mu = 2\zeta(2) - \zeta(4)$ ensues if the cascade is cut off at a fixed length $\bar{\eta}$, and $\mu = 2 - \zeta(6)$ (see [24]) if the cascade is terminated according to a local, fluctuating Reynolds number.

We also demonstrate our $u(x)$ ensemble to be useful in the analysis of experimental data. Finally, it forms the basis of a series of investigations [25,26] in which the statistics is actually determined from the Navier-Stokes equation.

In Sec. II we introduce the two different versions of our model, a spatially coherent and a spatially fluctuating one. In Sec. III the eddy-energy distribution will be studied within the simpler coherent version; the spatially fluctuating version turns out to give the same distribution. This fluctuating version is considered in Sec. IV, where we calculate the dissipation field and discuss its scaling properties. We then (Sec. V) calculate the scale-independent moments $\langle\langle \epsilon^q \rangle\rangle / \langle\langle \epsilon \rangle\rangle^q$ and discuss their $\text{Re} \epsilon_\lambda$ dependence. Section VI is reserved for a discussion: We explain how specific flows can be described by the model, compare our results with the analysis of experiments, and comment on other theoretical works.

II. FOURIER-WEIERSTRASS MODELING OF THE EULER FIELD

We start from the ansatz

$$\begin{aligned} u(x) &= \sum_{l=-N_\eta}^{N_L} u^{(l)}(x) e^{i\lambda^{-l}x/L_0} + \text{c.c.} \\ &= \sum_{k \in K} u_k(x) e^{ikx}, \end{aligned}$$

$$K = \{\pm L_0^{-1} \lambda^{-N_L}, \dots, \pm L_0^{-1} \lambda^{N_\eta}\} \quad (2.1)$$

for a one-dimensional turbulent velocity field. Of course, $u_{-k}(x) = [u_k(x)]^*$. L_0 is a reference length scale, and

$\lambda > 1$ is a real scaling factor. We will mostly think of $u(x)$ as being a one-dimensional cut through a three-dimensional velocity field $\mathbf{u}(\mathbf{x})$. So $u(x)$ is understood to be, e.g., $u_1(x_1)$. This is a completely adequate description of most existing experimental data, which are obtained by measuring the velocity at a single point. According to the Taylor hypothesis [1], this gives a signal equivalent to a one-dimensional section of the velocity field. Nevertheless, our approach is not limited to one-dimensional signals. In fact, a three-dimensional version of (2.1) forms the basis of a recent analysis of the Navier-Stokes equation [25].

Equation (2.1) corresponds to a decomposition of the velocity field into contributions from different cascade levels l , running from $l = -N_\eta$ to N_L . The diameter of the eddies of level l is $2\pi L_0 \lambda^l$. The amplitudes $u_k(x)$ are supposed to be periodic with period $2\pi L_0 \lambda^{N_L}$. So formally the signal extends to infinity, but nevertheless we have introduced a largest-length scale $2\pi L = 2\pi L_0 \lambda^{N_L}$. The diameter of the smallest eddies is $2\pi \bar{\eta}$ with $\bar{\eta} = L_0 \lambda^{-N_\eta}$. $\bar{\eta}$ obviously corresponds to a dissipation scale, at which the cascade is cut off by viscosity. The notation was introduced to keep $\bar{\eta}$ distinct from the usual Kolmogorov scale $\eta = (\nu^3/\epsilon)^{1/4}$.

Functions of the form (2.1) with $u^{(l)}(x) = \lambda^{-l\alpha}$, $0 < \alpha < 1$, and $N_\eta \rightarrow \infty$ were first considered by Weierstrass [27,28] to construct continuous functions that are nowhere differentiable. Physically, this corresponds to the fact that velocity gradients increase if finer and finer scales are resolved. In nature, N_η certainly is always finite, though Richardson [29] originally introduced (2.1) into turbulence theory to raise the question of nondifferentiability.

$u^{(l)}(x)$ represents the amplitude of an eddy of level l at position x . We shall take $u^{(l)}(x)$ to be constant over each eddy diameter $2\pi L_0 \lambda^l$ and assume $\lambda = 2$ for simplicity. There are $2^{N_L - l}$ eddies of this diameter on level l , $-N_\eta \leq l \leq N_L$. So we get a Cayley-tree-like structure [15] as depicted in Fig. 1. This structure is very similar

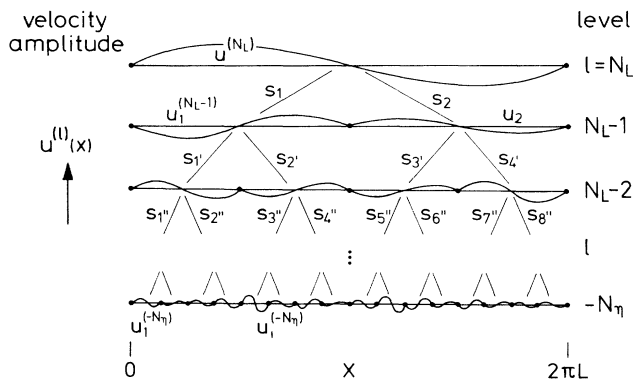


FIG. 1. The hierarchical structure of our eddy cascade. The amplitude of the largest eddy is $u_1^{(N_L)}$. It decays into two eddies with amplitudes $u_1^{(N_L-1)}$ and $u_2^{(N_L-1)}$. The decay process is described by the contraction factors s_1 and s_2 , $u_1^{(N_L-1)} = s_1 u_1^{(N_L)}$ and $u_2^{(N_L-1)} = s_2 u_1^{(N_L)}$. With $u_1^{(N_L-1)}$ and $u_2^{(N_L-1)}$ one then proceeds in the same way, etc.

to the multifractal models for the energy dissipation [11–13]. The amplitudes of the eddies of level l will be denoted by $u_i^{(l)}$, $i = 1, \dots, 2^{N_L - l}$. We introduce a stochastically self-similar structure on this hierarchy of eddies by specifying an ensemble for the $u_i^{(l)}$ in the following way: Let the amplitude $u_1^{(N_L)}$ of the largest eddy be u_L . The amplitudes $u_1^{(N_L-1)}$ and $u_2^{(N_L-1)}$ of the two eddies of the next smaller generation are obtained by multiplication with contraction factors s_1 and s_2 . Proceeding in the same way down the cascade, $u_i^{(l)}$ is given by $su_j^{(l+1)}$, where $u_j^{(l+1)}$ is the eddy that generates $u_i^{(l)}$. The contraction factors $s < 1$ are assumed to be random. They are chosen from a common probability distribution $p(s)$, since we assume all the various transitions as independent. This assures statistical self-similarity for the velocity field like in the cascade models for the dissipation field [11].

Two alternative models are considered. In the first one, termed “monofractal,” $u^{(l)}(x)$ is assumed to be totally independent of x , so all $u_i^{(l)} \equiv u^{(l)}$ are the same. One then has to choose only one single contraction factor s and $u^{(l)} = su^{(l+1)}$.

In the other, called the “multifractal” model, the different offsprings $u_i^{(l)}$ of each $(l+1)$ eddy are obtained with independently chosen s . So these models mark two different extremes: in the monofractal case there is one coherent plane wave in the whole volume for each level l , i.e., the eddy decay is spatially completely correlated within one level; in the multifractal model the mode amplitudes $u_i^{(l)}$ of the plane waves in each sub-box are statistically uncorrelated for $i_1 \neq i_2$; thus we have spatial fluctuations and only statistical spatial homogeneity. Our terminology is motivated by the nature of the measure generated by the corresponding ϵ field. As we will see in Sec. IV, the monofractal case corresponds to a space-filling ϵ measure, thus characterized by a single, in this case trivial, fractal dimension $D = 3$ (cf. [17]). In the multifractal case, the nonlinear function $\zeta(m)$ generates an infinity of exponents or “generalized dimensions” of the ϵ measure. This corresponds exactly to the usual terminology [12,30].

The complex amplitudes u_L of the largest eddy are distributed according to an independent probability distribution, which describes the statistics of the large-scale flow. Single brackets $\langle \rangle$ indicate the statistical averaging in the ensembles of the $u_i^{(l)}$ and of u_L . The distribution $p(s)$ carries all the information on the fragmentation process of the eddies, which dynamically would be dictated by the Navier-Stokes equation. Figure 2 gives an idea of how a typical velocity signal looks in the multifractal model. The specific distribution $p(s)$ we used will be given and motivated in Sec. III.

III. THE STRUCTURE FUNCTIONS

In this section we shall consider the spatially coherent monofractal case, where the amplitudes $u^{(l)}(x) = u^{(l)}$ are independent of x . Hence we have

$$u(x) = \sum_{l=-N_\eta}^{N_L} u^{(l)} e^{i\lambda^{-l}x/L_0} + \text{c.c.} \quad (3.1)$$

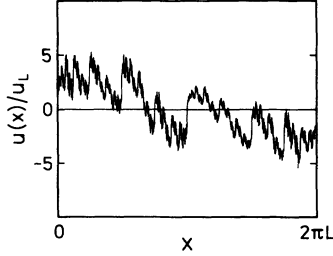


FIG. 2. A typical velocity signal as given by (2.1). The $u^{(l)}(x)$ are chosen according to the multifractal model. Parameters are $N_L=5$ and $N_\eta=4$. The distribution $p(s)$ is defined by (3.11) with (3.12); see Sec. III for details. The smallest scale is $2^{-(N_L+N_\eta)}2\pi L$, thus hardly visible by eye ($2\pi L/512$).

The $u^{(l)}$ can be written

$$u^{(l)} = u_L \prod_{i=1}^{N_L-1} s_i. \quad (3.2)$$

In the representation (3.1) the ensemble of $u(x)$ fields is not strictly translationally invariant, so we take $u(x+y)$ and average on y , denoting this by a second bracket. The y average now ensures $\langle\langle u(x) \rangle\rangle = 0$, of course. We get for the structure function

$$D(r) = \langle\langle |u(x+r) - u(x)|^2 \rangle\rangle \\ = 4 \sum_{l=-N_\eta}^{N_L} \langle |u^{(l)}|^2 \rangle [1 - \cos(\lambda^{-l}r/L_0)]. \quad (3.3)$$

In three-dimensional turbulence, $D(r)$ corresponds to the longitudinal structure function $D_{\parallel}^{(2)}(r)$.

Let us first assume that the contraction factors s are all equal, i.e., that the distribution $p(s)$ is sharp,

$$p(s) = \delta(s - \lambda^{-1/3}). \quad (3.4)$$

We then get

$$D(r) = 4 \langle |u_L|^2 \rangle (L/L_0)^{-2/3} \\ \times \sum_{l=-N_\eta}^{N_L} \lambda^{2l/3} [1 - \cos(\lambda^{-l}r/L_0)], \quad (3.5)$$

which is displayed in Fig. 3. The expected classical $r^{2/3}$

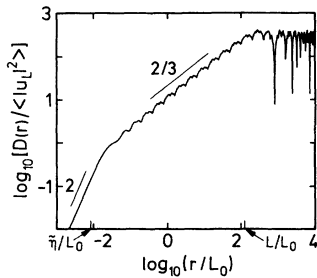


FIG. 3. The structure function $D(r)$ with sharp velocity scaling (3.4) according to (3.5). $D(r)$ is in units of the mean amplitude of the largest eddies, $\langle |u_L|^2 \rangle$. We have chosen $\lambda=2$ and $N_L=N_\eta=7$. This gives $L/L_0=128$, $\bar{\eta}/L_0=1/128$, and a scaling range $\bar{\eta}/L=6.1 \times 10^{-5}$.

dependence in the inertial subrange (ISR) $2\pi\lambda^{-N_\eta} \ll r/L_0 \ll 2\pi\lambda^{N_L}$ can be extracted from Eq. (3.5) analytically by performing the limits $N_L \rightarrow \infty$ and $N_\eta \rightarrow \infty$. Rescaling then the argument $r \rightarrow \lambda r$, one obtains

$$D(\lambda r) = \lambda^{2/3} D(r), \quad r \in \text{ISR}. \quad (3.6)$$

In the viscous subrange (VSR) $r \ll \bar{\eta}$, one may approximate in (3.3) $1 - \cos(\lambda^{-l}r/L_0)$ by $(\lambda^{-l}r)^2/2L_0^2$. Thus for $r \in \text{VSR}$

$$D(r) = 2 \left\langle \sum_{l=-N_\eta}^{N_L} \langle |u^{(l)}|^2 \rangle \lambda^{-2l} \right\rangle (r/L_0)^2 \propto r^2. \quad (3.7)$$

For $r \gtrsim L$, in the boundary subrange (BSR), the sum is dominated by the contribution of the largest eddies. The corresponding oscillations are visible in Fig. 3. $D(r)$ now depends on the large eddy shapes in a nonuniversal fashion. The three characteristic regimes of turbulent flow are thus built into our ansatz in a natural way.

Deviations from classical scaling appear if one allows the contraction factors to fluctuate. The exponents $\zeta(m)$ of the m th-order structure functions

$$D^{(m)}(r) = \langle\langle |u(x+r) - u(x)|^m \rangle\rangle \\ = \sum_{k_1 + \dots + k_n = 0} \langle \prod_{n=1}^m u_{k_n} (e^{ik_n r} - 1) \rangle \quad (3.8)$$

are calculated most easily by the saddle-point method [15]. The most significant contribution is obtained if $|k_n r| \approx 1$. Since the wave numbers k_n are $\pm \lambda^{-l}/L_0$, the saddle point $l=l_r$ is given by $r/L_0 \approx \lambda^{l_r}$ or $l_r \approx \ln(r/L_0)/\ln \lambda$, so $\langle \prod_{n=1}^m u_{k_n} \rangle = \langle u_L^m \rangle (\langle s^m \rangle)^{N_L - l_r}$.

Hence we have

$$D^{(m)}(r) \approx \langle u_L^m \rangle (r/L)^{\zeta(m)}, \quad (3.9)$$

$$\zeta(m) = \ln \langle s^m \rangle / \ln \lambda^{-1}. \quad (3.10)$$

In principle, every concave function $\zeta(m)$ can be realized by suitably choosing $p(s)$. Since $\zeta(3)=1$ is dictated by the Kolmogorov structure equation, one only has to ensure $\langle s^3 \rangle = \lambda^{-1}$.

We decided to use as a most simple $p(s)$ the bimodal distribution (and $\lambda=2$)

$$p(s) = p_a \delta(s - s_a) + p_b \delta(s - s_b), \quad (3.11)$$

and determined the free parameters p_a, s_a, s_b by a fit to the $\zeta(m)$, which are reported by Anselmet *et al.* [3] from their data analysis.

$$p_a = 0.65, \quad s_a = 0.71, \\ p_b = 1 - p_a = 0.35, \quad s_b = 0.91. \quad (3.12)$$

The bimodal distribution $p(s)$ determines the statistics of the velocity field itself instead of only the dissipation-rate distribution, as in Ref. [13]. As seen in Fig. 4, the fit is quite reasonable, but we attach no physical significance to the specific form (3.11) of $p(s)$.

Within our model, we have put all the dynamical infor-

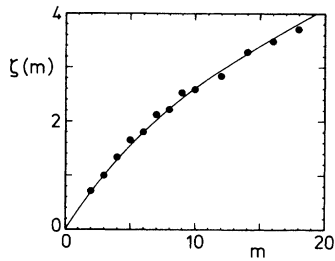


FIG. 4. The velocity moment scaling exponents $\zeta(m)$ as given by (3.10)–(3.12). The parameters $p_a=0.65$, $s_a=0.71$, $p_b=0.35$, $s_b=0.91$, and $\lambda=2$ were chosen to model the data of Anselmet *et al.* (dots) as closely as possible with our bimodal distribution (3.11). The constraint $\langle s^3 \rangle = \lambda^{-1}$ is satisfied.

mation on the fluctuating field into the parameters (3.12). Apart from N_L , N_η , and the large eddy amplitude u_L , these parameters will suffice to calculate any static quantity. Note that the monofractal model considered in this section already allows for an arbitrary spectrum of

velocity-scaling exponents. No x dependence and thus no spatial intermittency of the $u^{(l)}$ is necessary to obtain nonclassical $\zeta(m)$.

IV. DISSIPATION CORRELATIONS

A quantity of fundamental interest in turbulence is the dissipation field

$$\epsilon(x) = 15\nu \left[\frac{du(x)}{dx} \right]^2. \tag{4.1}$$

The prefactor 15 was chosen to define $\epsilon = \langle\langle \epsilon(x) \rangle\rangle$ equal to its usual value for a three-dimensional isotropic field. ν is still an arbitrary constant with the units of (length)²/(time). Since $u_k(x)$ is assumed to be locally constant we neglect its derivative, and from (2.1) we get

$$\epsilon(x) = -15\nu \sum_{k_1, k_2 \in K} u_{k_1}(x) u_{k_2}(x) k_1 k_2 e^{i(k_1+k_2)x}. \tag{4.2}$$

Its mean value is

$$\begin{aligned} \epsilon &= 30\nu L_0^{-2} \sum_{l=-N_\eta}^{N_L} \langle |u^{(l)}(x)|^2 \rangle \lambda^{-2l} = 30\nu L_0^{-2} \langle |u_L|^2 \rangle \sum_{l=-N_\eta}^{N_L} \lambda^{-2l} (\langle s^2 \rangle)^{N_L-l} \\ &= 30\nu L_0^{-2} \langle |u_L|^2 \rangle \lambda^{-2N_L} [(\lambda^2 \langle s^2 \rangle)^{N_L+N_\eta+1} - 1] / (\lambda^2 \langle s^2 \rangle - 1) \\ &= 30\nu \langle |u^{(-N_\eta)}|^2 \rangle \bar{\eta}^{-2} [\lambda^2 \langle s^2 \rangle - (\lambda^2 \langle s^2 \rangle)^{-N_L-N_\eta}] / (\lambda^2 \langle s^2 \rangle - 1). \end{aligned} \tag{4.3}$$

Equation (3.7) takes the form $D(r) = (\epsilon/15\nu)r^2$, as it should in the VSR. The dissipation field for the monofractal model is plotted in the upper part of Fig. 5. Obviously, the activity is evenly distributed, showing no intermittency. The reason is that (4.2) effectively represents a geometrical series, which would diverge if $N_\eta \rightarrow \infty$ and hence is dominated by the terms with $k_n = \pm \lambda^{N_\eta}/L_0$. So one mainly observes the sinusoidal oscillations of the smallest eddies. The scaling behavior is the same at any point as it should for a monofractal field. The lower part of Fig. 5 gives the dissipation field in the multifractal case; for comparison, an experimental field is reproduced in Fig. 6. The amplitudes $u_i^{(l)}$ were constructed as described in Sec. II. Our artificial signal exhibits the same impressively intermittent character as observed in experiments. It is therefore natural to look for the ϵ correlations:

$$\begin{aligned} C_\epsilon(r) &= \langle\langle \epsilon(x+r)\epsilon(x) \rangle\rangle \\ &= (15\nu)^2 \sum_{k_1+k_2+k_3+k_4=0} \langle u_{k_1}(x) u_{k_2}(x) u_{k_3}(x+r) u_{k_4}(x+r) \rangle k_1 k_2 k_3 k_4 e^{i(k_3+k_4)r}. \end{aligned} \tag{4.4}$$

The key observation is again that the terms $k_n = \pm \lambda^{N_\eta}/L_0 = \pm \bar{\eta}^{-1}$ dominate. Thus we can write

$$C_\epsilon(r) \approx (15\nu)^2 \bar{\eta}^{-4} (4 \langle |u^{(-N_\eta)}(x)|^2 |u^{(-N_\eta)}(x+r)|^2 \rangle + 2 \langle \{ u^{(-N_\eta)}(x) [u^{(-N_\eta)}(x+r)]^* \}^2 \rangle \cos(2r/\bar{\eta})). \tag{4.5}$$

At inertial range scales $r \gg \bar{\eta}$ the second term oscillates very fast and therefore does not enter the average dependence of $C_\epsilon(r)$ on r . The remaining task is to calculate $\langle |u^{(l)}(x)|^q |u^{(l)}(x+r)|^q \rangle$. This correlation function has been studied extensively, both analytically and numerically, by several authors [32–34]. The basic idea in evaluating it is that the length r fixes a cascade level $l_r = \log_\lambda(r/2\pi L_0)$, above which the contraction factors at x and $x+r$ are the same, while they are different for lower levels. Therefore, every level between l_r and N_L

contributes a factor $\langle s^{2q} \rangle$, and the levels between $-N_\eta$ and l_r give a factor $\langle s^q \rangle^2$. Thus we obtain

$$\begin{aligned} \langle |u^{(l)}(x)|^q |u^{(l)}(x+r)|^q \rangle \\ \approx \langle |u_L|^{2q} \rangle \langle s^{2q} \rangle^{N_L-l_r} (\langle s^q \rangle^2)^{l_r-l}. \end{aligned} \tag{4.6}$$

The x dependence is irrelevant for the scale dependence on r , as shown in [34], since the fields at x and $x+r$ are raised to the same power q .

Of course, the exponent $l_r - l$ is 0 if r is less than the l -

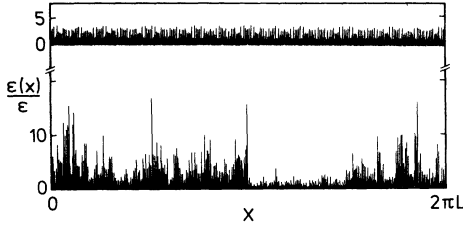


FIG. 5. Upper: The normalized dissipation field $\epsilon(x)/\langle\langle\epsilon(x)\rangle\rangle$ in the monofractal version of our model. We chose $N_L=5$ and $N_\eta=4$, corresponding to a Taylor-Reynolds number of about 1000; see Sec. VI. The amplitudes $u^{(l)}$ of the eddies of level l are given by $u^{(l)}=u_L\prod_{n=1}^{N_L-l} s_n$, with the s_n randomly chosen according to our standard distribution (3.11) and (3.12). Lower: The normalized dissipation field $\epsilon(x)/\langle\langle\epsilon(x)\rangle\rangle$ for the multifractal model. Parameters are the same, but now the amplitudes $u_i^{(l)}$ of the eddies are chosen independently.

eddy size, and N_L-l , is 0 if r is larger than $2\pi L$. Substituting (4.6) into (4.5) finally leads to

$$C_\epsilon(r) \approx 4(15\nu)^2 \bar{\eta}^{-4} \langle |u_L|^4 \rangle \langle s^4 \rangle^{N_L-l} (\langle s^2 \rangle)^{l+N_\eta}. \quad (4.7)$$

As we will show below, the scaling of the structure functions $D^{(m)}(r)$ is the same in the mono- or multifractal case. So (3.9) with (3.10) remain valid and we have from (4.7) $C_\epsilon(r) \propto r^{\zeta(4)-2\zeta(2)}$, giving the scaling relation

$$\mu = 2\zeta(2) - \zeta(4). \quad (4.8)$$

The same relation has already been conjectured by Nelkin and Bell [18]. It differs from the Kolmogorov-Obukhov 1962 scaling, where $\zeta(m) = m/3 - \mu m(m-3)/18$ implies $2\zeta(2) - \zeta(4) = (4/9)\mu$. Since $\zeta(m)$ is concave, one always has $\mu \geq 0$. For classical scaling, $\zeta(m)$ is a linear function of m and therefore $\mu = 0$. In the monofractal model $u^{(l)}(x)$ is independent of x , so $C_\epsilon(r)$ does not depend on r and $\mu = 0$ irrespective of $\zeta(m)$, following classical scaling or not.

To confirm our statement that the velocity scaling is not altered by multifractality, we consider the second-order structure function

$$D^{(2)}(r) = 4 \sum_{l=-N_\eta}^{N_L} \langle |u^{(l)}(x)|^2 \rangle \times \left[1 - \frac{\langle u^{(l)}(x+r)[u^{(l)}(x)]^* \rangle}{\langle |u^{(l)}(x)|^2 \rangle} \times \cos(\lambda^{-l}r/L_0) \right]. \quad (4.9)$$

Here we can safely neglect the x dependence of the $\langle u^{(l)}(x+r)[u^{(l)}(x)]^* \rangle$ correlation function as before. For $l > l_r$ we have $\langle u^{(l)}(x+r)[u^{(l)}(x)]^* \rangle = \langle |u^{(l)}(x)|^2 \rangle$, so the sum converges in both the $N_L \rightarrow \infty$ and $N_\eta \rightarrow \infty$ limits. Consequently we find a saddle point near $l = l_r$ as before giving $D^{(2)}(r) \approx \langle |u_L|^2 \rangle (r/L_0)^{\zeta(2)}$. The same arguments also apply to the higher-order structure functions.

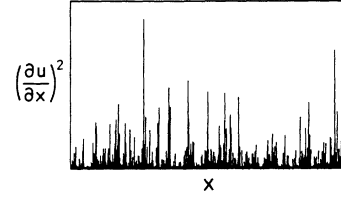


FIG. 6. The measured dissipation field in the turbulent wake of a cylinder [31]. The Taylor-Reynolds number in this experiment is only about 90 according to [23].

We conclude that the scaling of the $u(x)$ and $\epsilon(x)$ fields is governed by two completely different mechanisms: The structure functions $D^{(m)}(r)$ are dominated by eddies of typical size r . Although larger eddies have larger amplitudes, they simply convect both points x and $x+r$, so their contributions drop out of the velocity differences. By varying r , one thus probes the vertical structure of the hierarchy. In the $\epsilon(x)$ field, on the other hand, the contributions of the smallest eddies are most important, since they have the highest velocity gradients. So the ϵ correlation mainly gives information about the spatial structure of the smallest eddies.

V. ONE-POINT MOMENTS

We first study the scale-independent moments of ϵ . For q a natural number we have

$$\langle\langle \epsilon^q(x) \rangle\rangle = (-15\nu)^q \sum_{\substack{k_1, \dots, k_{2q} \\ \sum_n k_n = 0}} \langle \prod_{n=1}^{2q} u_{k_n} \rangle.$$

Making the usual approximation $k_n = \pm \bar{\eta}^{-1}$, this gives

$$\langle\langle \epsilon^q(x) \rangle\rangle \approx (15\nu)^q [(2q)!/(q!)^2] \times \langle |u^{(-N_\eta)}|^{2q} \rangle \bar{\eta}^{(-2q)},$$

which leads [with (3.10)] to

$$\frac{\langle\langle \epsilon^q \rangle\rangle}{\langle\langle \epsilon \rangle\rangle^q} \propto \frac{\langle |u^{(-N_\eta)}|^{2q} \rangle}{\langle |u^{(-N_\eta)}|^2 \rangle^q} \propto \frac{\langle s^{2q} \rangle^{N_L+N_\eta}}{\langle s^2 \rangle^{q(N_L+N_\eta)}} \propto \left[\frac{\bar{\eta}}{L} \right]^{\zeta(2q) - q\zeta(2)}. \quad (5.1)$$

We now have to relate $(\bar{\eta}/L)$ to Re_λ . To that end some other moments are needed. Using again (3.10) and taking the limit $N_L + N_\eta \rightarrow \infty$ (more precisely, $\langle s^2 \rangle^{N_L+N_\eta+1} \ll 1$),

$$\langle\langle u^2 \rangle\rangle = 2 \langle |u_L|^2 \rangle \sum_{l=-N_\eta}^{N_L} \langle s^2 \rangle^{N_L-l} = 2 \langle |u_L|^2 \rangle (1 - \lambda^{-\zeta(2)})^{-1}. \quad (5.2)$$

$$\left\langle\left\langle \left[\frac{du}{dx} \right]^2 \right\rangle\right\rangle = 2 \langle |u_L|^2 \rangle L^{-\zeta(2)} \bar{\eta}^{\zeta(2)-2} \times (1 - \lambda^{\zeta(2)-2})^{-1}. \quad (5.3)$$

These moments already allow us to calculate the Taylor microscale

$$\lambda_T = \left[\frac{\langle\langle u^2 \rangle\rangle}{\langle\langle (du/dx)^2 \rangle\rangle} \right]^{1/2} = \left[\frac{1 - \lambda^{\zeta(2)-2}}{1 - \lambda^{-\zeta(2)}} \right]^{1/2} L^{\zeta(2)/2} \tilde{\eta}^{2-\zeta(2)/2}. \tag{5.4}$$

Since $\langle\langle (du/dx)^2 \rangle\rangle = \epsilon/15\nu$, one also obtains by solving for ν an expression for $\eta = (\nu^3/\epsilon)^{1/4}$,

$$\eta = [(\epsilon L)^{2/3} \langle |u_L|^2 \rangle^{-1} L^{\zeta(2)-2/3} \tilde{\eta}^{2-\zeta(2)} \times (1 - \lambda^{\zeta(2)-2})/30]^{3/4}. \tag{5.5}$$

One expects the dimensionless combination $\langle |u_L|^2 \rangle / (\epsilon L)^{2/3}$ to be Re_λ -number independent, since the mean amplitude $\langle |u_L|^2 \rangle^{1/2}$ of the largest eddies is unaffected by the eddy decay. It should therefore be independent of the length of the cascade. We relate $\langle |u_L|^2 \rangle / (\epsilon L)^{2/3}$ to the amplitude b_\parallel in

$$D_\parallel^{(2)}(r) = b_\parallel (\epsilon r)^{2/3} (r/L)^B \tag{5.6}$$

via the Poisson summation formula [35]

$$\sum_{l=-\infty}^{\infty} \lambda^{\alpha l} [1 - \cos(\lambda^{-l} r/L_0)] = \text{Re} \left\{ \frac{e^{i\pi(2-\alpha)/2}}{\ln \lambda} \sum_{n=-\infty}^{\infty} e^{-2\pi i n \log_\lambda r} e^{-\pi^2 n / \ln \lambda} \times \Gamma(-\alpha + i2\pi n / \ln \lambda) \right\} \times \left[\frac{r}{L_0} \right]^\alpha.$$

Taking only the $n=0$ term into account, we get from (3.3) apart from small oscillatory corrections $D(r) = 4\Lambda \langle |u_L|^2 \rangle (r/L)^{\zeta(2)}$ with $\Lambda = \Gamma(1 - \zeta(2)) \cos[\pi\zeta(2)/2] / \zeta(2) \ln \lambda$. Comparison with (5.6) gives $B + \frac{2}{3} = \zeta(2)$,

$$b_\parallel = 4\Lambda \langle |u_L|^2 \rangle / (\epsilon L)^{2/3}, \tag{5.7}$$

and (5.5) simplifies to

$$\eta = \{ [4\Lambda(1 - \lambda^{\zeta(2)-2}) / 30 b_\parallel] (L/\tilde{\eta})^{\zeta(2)-2/3} \}^{3/4} \tilde{\eta}. \tag{5.8}$$

So in the presence of intermittency, $\zeta(2) > 2/3$, η and $\tilde{\eta}$ define two different types of scales, as already observed by Mandelbrot [36]. As the Re number is increased, $L/\tilde{\eta} \gg 1$, and eventually $\eta \gg \tilde{\eta}$. So, in principle, the cascade may extend far beyond the Kolmogorov scale η .

The Taylor Re number is defined as

$$Re_\lambda = \lambda_T \langle\langle u^2 \rangle\rangle^{1/2} / \nu = \langle\langle u^2 \rangle\rangle / \langle\langle (u')^2 \rangle\rangle^{1/2} \nu = \sqrt{15} \langle\langle u^2 \rangle\rangle / (\epsilon \nu)^{1/2} = \sqrt{15} \langle\langle u^2 \rangle\rangle / (\epsilon \eta)^{2/3}.$$

Using (5.7) and (5.2) this gives

$$Re_\lambda = [\sqrt{15}/2\Lambda(1 - \lambda^{-\zeta(2)})] b_\parallel (L/\eta)^{2/3}. \tag{5.9}$$

Inserting (5.5) into (5.9) finally leads to

$$Re_\lambda = (b_\parallel/2\Lambda)^{3/2} [15/(1 - \lambda^{-\zeta(2)})(1 - \lambda^{\zeta(2)-2})^{1/2}] \times (L/\tilde{\eta})^{1-\zeta(2)/2}. \tag{5.10}$$

We now combine (5.1) and (5.10), which gives for $g(q)$ defined in Eq. (1.16)

$$g(q) = 2[q\zeta(2) - \zeta(2q)] / [2 - \zeta(2)]. \tag{5.11}$$

It is a straightforward consequence of our model that the skewness

$$S = 3 \sum_{l=-N_\eta}^{N_\eta-1} \lambda^{-3l-2} \text{Im} \{ \langle u^{(l)} [u^{(l+1)}]^2 \rangle^* \}$$

scales with Re_λ in the same way as $\langle\langle \epsilon^{3/2} \rangle\rangle / \langle\langle \epsilon \rangle\rangle^{3/2}$. One only has to choose the distribution of u_L such that $\text{Im} \{ \langle u_L (u_L^2)^* \rangle \}$ is negative. This ensures $S < 0$, as required by the Kolmogorov structure equation; see (6.7) below. Therefore, continuing (5.11) to nonintegral q , we get for the exponents of skewness and kurtosis

$$\mu_S = [3\zeta(2) - 2\zeta(3)] / [2 - \zeta(2)] \tag{5.12}$$

and

$$\mu_K = [4\zeta(2) - 2\zeta(4)] / [2 - \zeta(2)] = 2\mu / [2 - \zeta(2)]. \tag{5.13}$$

The formulas given in this section now allow one to calculate various physical quantities (such as ϵ , λ_T , and Re_λ) once the model parameters N_L , N_η , $(T_0/L_0)^2 \langle |u_L|^2 \rangle$, and $p(s)$ are specified. As the time scale T_0 we take L_0^2/ν , since ν is a given constant characterizing a fluid. All the other quantities adjust themselves when the boundary conditions are specified and thus characterize the flow.

VI. DISCUSSION

First we outline how our model can describe the velocity signal of a specific flow. Typical quantities given from experiment are

$$\eta, \lambda_T, \zeta(m), \text{ and } b_\parallel. \tag{6.1}$$

η and λ_T characterize the flow, whereas $\zeta(m)$ and b_\parallel are supposed to be universal. The model parameters we wish to calculate from (6.1) are

$$N_L, N_\eta, (L_0/\nu)^2 \langle |u_L|^2 \rangle, \text{ and } p(s). \tag{6.2}$$

$p(s)$ is defined by its moments $\langle s^m \rangle = \lambda^{-\zeta(m)}$. For most practical purposes, we may take $\zeta(2) = \frac{2}{3}$ in the formulas of Sec. V. By virtue of (5.7) and (5.3), $(L_0/\nu)^2 \langle |u_L|^2 \rangle$ can be calculated from N_L and N_η using the value $b_\parallel = 2.3$ for the universal constant b_\parallel . This value was obtained from a least-squares fit to available experimental data [2]. If the scaling parameter is chosen as $\lambda = 2$ we have

$$(L_0/\nu)^2 \langle |u_L|^2 \rangle = 19.3 \times 2^{2(4N_\eta + N_L)/3}. \tag{6.3}$$

So only N_L and N_η have to be adjusted to a specific flow. This is done using

TABLE I. This table compiles various numbers characteristic of the turbulent state. The data for the duct flow are from [3], Table 1, for the atmospheric flow from [37], Table 1, Run 16. The values for N_L and N_η are calculated from this data via (6.4) with $L_0=1$ cm. In turn, given N_L and N_η , all quantities above them in the Table can be calculated (in units of L_0 and L_0^2/ν) using (6.3) and (5.2)–(5.10). In this sense our Fourier-Weierstrass model describes realistic velocity signals of high-Re-number flow.

Quantity (units)	Duct flow	Atmospheric flow
ϵ (cm ² s ⁻³)	1.12×10^5	740
ν (cm ² s ⁻¹)	0.147	0.149
η (cm)	0.013	0.046
v_η (cm s ⁻¹)	35.8	3.24
$(\langle\langle u^2 \rangle\rangle)^{1/2}$ (cm s ⁻¹)	169	143
$(\langle\langle u'^2 \rangle\rangle)^{1/2}$ (s ⁻¹)	225	18.6
λ_T (cm)	0.75	7.7
Re_λ	852	7353
N_L	5	12
N_η	4	2

$$\eta/L_0 = 0.18 \times 2^{-N_\eta}, \quad \lambda_T/L_0 = 4.01 \times 2^{N_L/3 - 2N_\eta/3}, \quad (6.4)$$

which follow from (5.8) and (5.4). We note some flow characteristics, together with the corresponding model parameters, for two different experiments in Table I. The data of the first and second columns are from [3] and [37], respectively.

We now discuss the different scaling relations for μ , μ_S , and μ_K . As mentioned in the Introduction, we have also studied [24] a refined version of the model presented here. Instead of fixing a cutoff scale $\tilde{\eta}$, the cascade is terminated at the level N_x at which the local Re number

$$Re_x = u^{(-N_x)}(x) L_0 \lambda^{-N_x} / \nu \quad (6.5)$$

reaches a critical value Re_{cr} . Thus the cutoff scale η_x will

in general fluctuate between different realizations of $u(x)$ as well as in space. Its average value $\langle \eta_x \rangle$ is proportional to the Kolmogorov length η . If the eddies are spatially independent, we find $\mu = 2 - \zeta(6)$ as in the Obukhov theory. Perfect spatial coherence again leads to $\mu = 0$, of course. Nelkin [38] studies a fractal model in much the same spirit, and finds

$$\mu_S = 9\mu/16, \quad \mu_K = 3\mu/2 \quad (6.6)$$

to lowest order in μ , in agreement with our own results [24]. Note that the scaling relations obtained for the fluctuating cutoff theory do not rely on dimensional arguments like the Obukhov theory [4,17,39], presented in the Introduction. Nelkin also makes the interesting observation that the relation

$$\langle (\partial_1 u_1)^3 \rangle = -2\nu \langle (\partial_1^2 u_1)^2 \rangle, \quad (6.7)$$

which follows from the Kolmogorov structure equation, puts constraints on turbulence models. Specifically, our constant cutoff assumption can only be approximately valid, since it can be shown to violate (6.7). On the other hand, (6.7) can easily be satisfied with an appropriate choice of Re_{cr} in the version with fluctuating cutoff.

In Table II we document how the scaling relations (4.8), (5.12), and (5.13) compare with direct experimental measurements of μ , μ_S , and μ_K , and the results of the fluctuating cutoff theory (1.11) and (6.6). The necessary values of $\zeta(m)$ are taken from the (3.10)–(3.12) interpolation of the empirical values obtained by analyzing velocity signals of real flows. The measurements seem to support the fluctuating cutoff theory. But in view of the available data, it seems fair to say that this support is not very conclusive. For example, μ depends heavily on the kind of correlation function used. The value of 0.18 given in the table is based on $\langle\langle \epsilon(\mathbf{x}, t) \epsilon(\mathbf{x} + \mathbf{r}, t) \rangle\rangle$ (as is our calculation of μ), whereas 0.48 is obtained [3] if the centered correlation function is used, as in (1.10). Moreover, μ depends sensitively on the choice of the inertial range. The data of Van Atta and Antonia [40] collected from many different experiments, show so much scatter

TABLE II. Here we give some exponents that characterize the ϵ fluctuations. μ is the exponent of the ϵ correlations and μ_S and μ_K describe the Re_λ -number dependence of skewness and kurtosis, respectively. μ as quoted in the first line was taken from [3], μ_S and μ_K from [40]. These exponents represent the analysis of the available data. The second line summarizes the results of the fluctuating cutoff theory [4,24,38] [scaling relations (1.11) and (6.6)] with $\zeta(m)$ from (3.10)–(3.12), which fit the empirical values from analyzing the data [3]. The third line stems from our scaling relations (4.8), (5.12), and (5.13), with $\zeta(m)$ also according to (3.10)–(3.12).

Dissipation exponent	μ	μ_S	μ_K	μ/μ_K	μ_S/μ_K
From data analysis	0.18	0.15	0.41	0.44	0.37
Fluctuating cutoff theory	0.20	0.11	0.30	0.67	0.38
Constant cutoff theory	0.09	0.05	0.14	0.66	0.39

that they also seem to be consistent with much lower values for μ_S and μ_K . Somewhat arbitrarily, only the data with $\text{Re}_\lambda > 500$ are used for the fit.

On the other hand, if the older empirical values of Van Atta and Park [41,42] are used for $\zeta(m)$, our theory agrees very well with the direct measurements of μ . They report $\mu=0.5$ and the fit $\zeta(m)=m/3-\mu m(m-3)/18$. This gives $\mu=0.22$ with our scaling relation (4.8) instead of $\mu=0.09$, and $\mu_S=0.13$, $\mu_K=0.35$ from (5.12) and (5.13), all rather near the values of the Obukhov theory and of experiments.

We already stressed the fact that once a $u(x)$ ensemble is specified, the scaling relations between the u and ϵ fluctuations are fixed. The monofractal and the multifractal versions of our model led to different scaling relations. It seems reasonable to believe that there is some correlation between the eddies of the same generation l without enjoying complete coherence, i.e., the correct scaling relation might be between (1.11) and $\mu=0$. But clearly we must conclude that a detailed knowledge of the underlying dynamics is necessary to make reliable scaling predictions.

We investigated the dynamical implications of our model in two recent papers [25,26]. A three-dimensional version of both the monofractal [25] and the multifractal [26] model was inserted into the Navier-Stokes equation. This results in dynamical equations for the coefficients $u_k(x)$. Keeping only interactions between neighboring levels, these sets of equations constitute approximate solutions of the Navier-Stokes equation. The statistics of $u_k(x)$ can now be inferred from the Navier-Stokes generated dynamics.

In the monofractal case we have $\mu=0$, of course, but in principle exponent deviations $\delta\zeta(m)\neq 0$ are consistent with this, as shown above. Nevertheless, we found self-similarity, but also $\delta\zeta(m)=0$ within the error of our calculation. Therefore, the dynamical origin of $\delta\zeta(m)\neq 0$ must be sought in a spatial variation of $u_k(x)$, as in our multifractal model. In fact, in our dynamical counterpart [26] of the multifractal model, we now found appreciable corrections $\delta\zeta(m)\neq 0$. Due to the nature of the approximations made, we were so far not able to study the ϵ fluctuations independently. Hence investigations of the type performed here give very important complementary information on the nature of the cascade.

Many of the conclusions drawn here are also contained in a paper by Kraichnan [43]. Specifically, he noticed that $\epsilon_r(\mathbf{x},t)\approx\epsilon$, $r\in\text{ISR}$, as in our monofractal model, is consistent with large fluctuations in the energy transfer (cf. Sec. II of his paper). This means that $\mu=0$ is consistent with $\delta\zeta(m)\neq 0$. To support this view, Kraichnan gave plausible arguments, but did not use a specific model that really verifies it, as we did.

Recently, Yakhot, Orszag, and She [44] derived still another scaling relation,

$$\mu=2-3\zeta(2), \quad (6.8)$$

for the Navier-Stokes equation with external Gaussian white noise coupled to it. The external force was as-

sumed to correlate as

$$\langle f_i(\mathbf{p},t)f_j(\mathbf{p}',t') \rangle = 2D_0|\mathbf{p}|^{-3+\mu/2}(2\pi)^d \mathbf{p}_{ij}^{\perp}(\mathbf{p}) \times \delta(\mathbf{p}+\mathbf{p}')\delta(t-t'). \quad (6.9)$$

The exponent $-3+\mu/2$ was chosen to ensure $\langle \epsilon(\mathbf{x}+\mathbf{r},t)\epsilon(\mathbf{x},t) \rangle \propto r^{-\mu}$. From (6.9), $\zeta(2)$ can be calculated exactly [45] to give (6.8).

We want to demonstrate that (6.8) is not due to fluctuations, but solely results from the specific form of the energy input. This type of correction is thus beyond the aim of the present model. From the Navier-Stokes equation with an external force one can easily derive an analogue of the Kolmogorov structure equation [1]

$$D_{\parallel}^{(3)}(r)-6\nu\partial_r D_{\parallel}^{(2)}(r) = -\frac{12}{r^4} \int_0^r r'^4 \dot{E}_{\parallel}(r') dr'. \quad (6.10)$$

Here \dot{E}_{\parallel} is the energy input rate per unit mass,

$$\dot{E}_{\parallel}(r) = \langle f_i(\mathbf{x},t)u_j(\mathbf{x}+\mathbf{r},t) \rangle r_i r_j / r^2. \quad (6.11)$$

If the energy is fed in only on the largest scales, $\dot{E}_{\parallel}(r)$ is constant and $\dot{E}_{\parallel}(r) = \langle f_i(\mathbf{x},t)u_i(\mathbf{x},t) \rangle / 3 = \epsilon/3$. This gives $D_{\parallel}^{(3)} \propto r$ irrespective of any fluctuations. For the force (6.9), by contrast, we find within standard Langevin theory [46]

$$\langle f_i(\mathbf{p},t)u_i(\mathbf{p}',t) \rangle = (d-1)D_0|\mathbf{p}|^{-3+\mu/2} \times (2\pi)^d \delta(\mathbf{p}+\mathbf{p}'). \quad (6.12)$$

The energy input rate into one wave-number octave $p/\sqrt{2} \leq k \leq p\sqrt{2}$ increases with p as $p^{\mu/2}$, since the number of modes within the octave increases as p^3 . Therefore, the energy is favorably fed in at the smallest scales. Inserting (6.12) into (6.9) gives $D_{\parallel}^{(3)}(r) \propto r^{1-\mu/2}$, in contrast to our usual assumption $\zeta(3)=1$.

In our Navier-Stokes-based Fourier-Weierstrass analysis of high-Re-number flow [25] we did not couple external noise. There is no relation like (6.9). Instead, the fluctuations are purely due to the nonlinear character of the dynamical equations, i.e., they are deterministic chaotic.

Let us summarize our results as follows: To date, all existing theories connecting velocity and dissipation correlations are based on dimensional arguments generalizing the classical theories of the 1940s. Instead, we introduced a model that allows for a consistent derivation of the relevant scaling relations. It is based as closely as possible on the properties of the velocity field itself and on popular notions about the origin of intermittency. This means that intermittency is traced back to the fluctuations involved in a succession of eddy decays of the velocity field. So we are able to disentangle the mechanisms that produce velocity and dissipation correlations. Nevertheless, there is ample freedom to define different models, so that one really has to consider the underlying dynamics. One might even say that further progress in turbulence theory without specific reference to the Navier-Stokes equation will be illusory.

- [1] A. S. Monin and A. M. Yaglom, *Statistical Fluid Mechanics* (MIT, Cambridge, MA, 1971), Vol. II.
- [2] H. Effinger and S. Grossmann, *Z. Phys. B* **66**, 289 (1987).
- [3] F. Anselmet, Y. Gagne, E. J. Hopfinger, and R. A. Antonia, *J. Fluid Mech.* **140**, 63 (1984).
- [4] A. M. Obukhov, *J. Fluid Mech.* **13**, 77 (1962).
- [5] A. N. Kolmogorov, *C. R. Acad. Sci. USSR* **30**, 299 (1941).
- [6] A. M. Obukhov, *C. R. Acad. Sci. USSR* **32**, 19 (1941).
- [7] C. F. von Weizsäcker, *Z. Phys.* **124**, 614 (1948).
- [8] W. Heisenberg, *Z. Phys.* **124**, 628 (1948).
- [9] L. Onsager, *Phys. Rev.* **68**, 286 (1945).
- [10] A. N. Kolmogorov, *J. Fluid Mech.* **13**, 82 (1962).
- [11] B. B. Mandelbrot, *J. Fluid Mech.* **62**, 331 (1974).
- [12] U. Frisch and G. Parisi, in *Turbulence and Predictability in Geophysical Fluid Dynamics and Climate Dynamics*, edited by M. Ghil, R. Benzi, and G. Parisi (North-Holland, New York, 1985), p. 84.
- [13] C. Meneveau and K. R. Sreenivasan, *Phys. Rev. Lett.* **59**, 1424 (1987).
- [14] A. M. Yaglom, *Dokl. Akad. Nauk SSSR* **166**, 49 (1966) [*Sov. Phys. Dokl.* **11**, 26 (1966)].
- [15] A. Erzan, S. Grossmann, and A. Hernandez-Machado, *J. Phys. A* **20**, 3913 (1987).
- [16] E. A. Novikov, *Phys. Fluids A* **2**, 814 (1990).
- [17] U. Frisch, P. L. Sulem, and M. Nelkin, *J. Fluid Mech.* **87**, 719 (1978).
- [18] M. Nelkin and T. L. Bell, *Phys. Rev. A* **17**, 363 (1978).
- [19] S. Grossmann and S. Thomae, *Z. Phys. B* **49**, 253 (1982).
- [20] H. G. E. Hentschel and I. Procaccia, *Phys. Rev. Lett.* **49**, 1158 (1982).
- [21] E. A. Novikov and R. W. Stewart, *Izv. Akad. Nauk SSSR, Ser. Geofiz.* **3**, 408 (1964).
- [22] R. Benzi, G. Paladin, G. Parisi, and A. Vulpiani, *J. Phys. A* **17**, 3521 (1984).
- [23] C. Meneveau and K. R. Sreenivasan, *Nucl. Phys. B (Proc. Suppl.)* **2**, 49 (1987).
- [24] J. Eggers and S. Grossman, *Phys. Lett. A* **153**, 12 (1991).
- [25] J. Eggers and S. Grossmann, *Phys. Fluids A* **3**, 1958 (1991).
- [26] J. Eggers and S. Grossmann, *Phys. Lett. A* **156**, 444 (1991).
- [27] M. V. Berry and Z. V. Lewis, *Proc. R. Soc. London, Ser. A* **370**, 459 (1980).
- [28] For references on the Weierstrass function, see B. B. Mandelbrot, *The Fractal Geometry of Nature* (Freeman, San Francisco, 1982).
- [29] L. F. Richardson, *Proc. R. Soc. London, Ser. A* **110**, 709 (1926).
- [30] T. C. Halsey, M. H. Jensen, L. P. Kadanoff, I. Procaccia, and B. I. Shraiman, *Phys. Rev. A* **33**, 1141 (1986).
- [31] K. R. Sreenivasan, R. Ramshankar, and C. Meneveau, *Proc. R. Soc. London, Ser. A* **421**, 79 (1989).
- [32] M. E. Cates and J. M. Deutsch, *Phys. Rev. A* **35**, 4907 (1987).
- [33] A. P. Siebesma and L. Pietronero, *J. Phys. A* **21**, 3259 (1988).
- [34] C. Meneveau and A. Chhabra, *Physica A* **164**, 564 (1990).
- [35] M. J. Lighthill, *Introduction to Fourier Analysis and Generalized Functions* (Cambridge University, Cambridge, England, 1958), p. 67.
- [36] B. B. Mandelbrot, in *Turbulence and the Navier-Stokes Equation*, edited by R. Temam, *Lecture Notes in Mathematics* Vol. 565 (Springer, Berlin, 1976).
- [37] R. A. Antonia, B. R. Satyaprakash, and A. J. Chambers, *Phys. Fluids* **25**, 29 (1982).
- [38] M. Nelkin, *Phys. Rev. A* **42**, 7226 (1990).
- [39] J. C. Wyngaard and H. Tennekes, *Phys. Fluids* **13**, 1962 (1970).
- [40] C. W. Van Atta and R. A. Antonia, *Phys. Fluids* **23**, 252 (1980).
- [41] C. W. Van Atta and J. Park, in *Statistical Models and Turbulence*, edited by M. Rosenblatt and C. W. Van Atta (Springer, Berlin, 1972), p. 402.
- [42] C. W. Van Atta and W. Y. Chen, *J. Fluid Mech.* **44**, 145 (1970).
- [43] R. H. Kraichnan, *J. Fluid Mech.* **62**, 305 (1974).
- [44] V. Yakhot, Z. S. She, and S. A. Orszag, *Phys. Fluids A* **1**, 289 (1989).
- [45] C. De Dominicis, and P. C. Martin, *Phys. Rev. A* **19**, 419 (1979).
- [46] H. Risken, *The Fokker-Planck Equation* (Springer-Verlag, Berlin, 1984).